Hybrid Platoon Control Based on Driving Characteristics

Jingpeng Hu[1,2(✉)] and Zhiguo Xiong[3]

[1] School of Computing, Beijing Institute of Technology, Zhuhai 519000, China
02092@bitzh.edu.cn
[2] Software Engineering Technology Research Center, Zhuhai 519000, China
[3] School of Aviation, Beijing Institute of Technology, Zhuhai 519000, China

Abstract. Research is being conducted on the problem of nonlinear cooperative formation control of unmanned vehicles, considering sensor failures. Firstly, a nonlinear cooperative control system model that incorporates sensor failures is being established. Secondly, a model predictive controller is being designed based on this model using the Lyapunov method and linear matrix inequalities (LMIs) to optimize the control performance metrics of the vehicle fleet. This approach ensures both the asymptotic stability and queue stability of the fleet while further enhancing its control performance. Lastly, the effectiveness and practicality of the algorithm are being validated through an experimental fleet constructed with Arduino serving as the control unit.

Keywords: Hybrid platoon system · Speed strategy · Driving characteristics · Integral event-triggered mechanism

1 Introduction

The development of the automotive industry and the acceleration of urbanization are leading to a rapid increase in vehicle ownership worldwide [1]. Current statistics indicate that the global registered motor vehicle count has exceeded one billion, with the number continuing to grow at a swift pace [2, 3]. As a result, various transportation system issues are arising, including traffic congestion, accidents, and environmental pollution. To tackle this problem, extensive research is being conducted by both domestic and international research teams on the cooperative formation control of unmanned vehicles in intelligent highway systems [4, 5]. This encompasses the investigation of lane-changing control systems, autonomous platooning systems, and cooperative adaptive cruise control systems for unmanned vehicles. These endeavors collectively contribute to the field of unmanned vehicle cooperative formation control technology [6].

Unmanned vehicle cooperative control facilitates the automatic formation of platoons in the highway system through wireless communication and sensing technologies [7]. Information exchange and speed adjustment occur among vehicles within the platoon, based on the states of neighboring vehicles, resulting in synchronized platoon systems

V. C. M. Leung et al. (Eds.): Qshine 2023, LNICST 574, pp. 346–359, 2024.
https://doi.org/10.1007/978-3-031-65123-6_25

[8]. Currently, researchers are conducting notable studies on cooperative formation control of unmanned vehicles [9]. In reference [1–4], an LQG controller is utilized to convert spatial constraints and velocity into lateral steering and longitudinal acceleration control, ensuring the safety and comfort of unmanned vehicle operation. Reference [5–9] addresses a nonlinear model of platoon systems composed of homogeneous unmanned vehicles by proposing a distributed H∞ control method, achieving stability and queue stability of the platoon system. Reference [10–12] introduces a global finite-time tracking control method that employs a discontinuous controller to achieve trajectory tracking in closed-loop autonomous driving systems. For lateral trajectory tracking control of unmanned vehicles, reference [13–16] designs a neural network PID controller, demonstrating algorithm feasibility through simulations. Moreover, fuzzy control theory has been effectively applied to nonlinear platoon control problems as evidenced in references [17–19]. Reference [20] focuses on designing optimal trajectories for unmanned vehicles in cooperative adaptive cruise control platoons. Experimental tests confirm the effectiveness of the proposed model in optimizing the trajectories of unmanned vehicles within the platoon.

The study of cooperative control for unmanned vehicles in academic research has predominantly focused on two key areas: (1) The platoon models commonly employed primarily utilize linear models in the longitudinal direction. However, in practical scenarios, unmanned vehicle models exhibit high levels of nonlinearity, particularly when considering the longitudinal-lateral coupling within the platoon model. Currently, there exists limited research in this specific domain. (2) Control method investigations generally assume accurate sensor measurements. Nevertheless, sensors are susceptible to disruptions from external environmental factors encountered in real-world situations, such as adverse weather conditions like rain, fog, or environments with low visibility. Infrared, radar, electromagnetic sensors, and others are prone to failures in such conditions. Considering these aspects, this study aims to address both the longitudinal-lateral coupling in the platoon model and the influence of sensor failures. A model predictive control method based on Linear Matrix Inequalities (LMI) will be developed to facilitate the achievement of safe and stable platoon operation.

2 Problem Description

In the context of the platoon system comprising n vehicles, it is assumed that the leading vehicle possesses the capability to transmit information to other vehicles, while the front vehicle has the ability to transmit information to adjacent following vehicles.

2.1 Nonlinear Platoon Modeling

The position and linear velocity of the $i(i = \mathrm{L}, 1 \cdots, n-1)$ vehicle in the absolute coordinate system are denoted by (x_i, y_i) and v_i, respectively, while the position of the lead unmanned vehicle is represented by (x_L, y_L). In this study, factors such as road slope or lateral displacement of the unmanned vehicles are not considered. It is assumed that both the front and rear wheels of each vehicle can be steered, and the steering angle is

denoted as θ_i. The following set of nonlinear differential equations can be used to model the kinematics of the i-th vehicle.

$$\begin{cases} \dot{x}_i = v_i \cos\theta_i \\ \dot{y}_i = v_i \sin\theta_i \\ \dot{\theta}_i = w_i \end{cases} \tag{1}$$

In above equation, θ_i represents the absolute heading angle, and w_i denotes the centroid angular velocity.

Based on the relative positions of unmanned vehicles on the horizontal plane, we can establish the platoon error model as follows:

$$\begin{cases} x_i^e = (x_{i-1} - x_i - \mathrm{l})\cos\theta_i + (y_{i-1} - y_i)\sin\theta_i \\ y_i^e = -(x_{i-1} - x_i)\sin\theta_i + (y_{i-1} - y_i)\cos\theta_i \\ \theta_i^e = -\theta_i + \theta_{i-1} \end{cases} \tag{2}$$

In Eq. (2), the relative distances along the x-axis and y-axis are represented by x_i^e and y_i^e, respectively, with respect to the preceding vehicle. The relative direction is denoted by θ_i^e, and $0 \le \theta_i < \pi/2$ represents a specific value. The straight-line distance between two adjacent vehicles is indicated by l, as illustrated in Fig. 1.

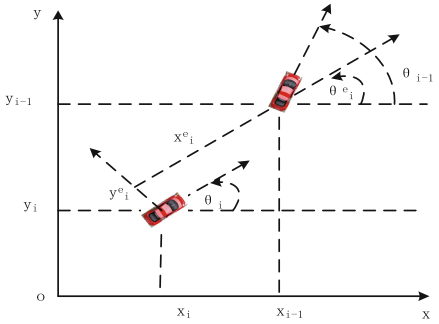

Fig. 1. The platoon model in a relative coordinate system

The nonlinear state space equation of the platoon system is obtained by deriving it from Eq. (2), which represents the derivative equation of the relative model.

$$\dot{X}_i(t) = F_i(X_i(t)) + G_i(X_i(t))u_i(t) \tag{3}$$

In above equation, the individual state of an unmanned vehicle in the fleet system is represented by $X_i(t) = \left[x_i^e \; y_i^e \; \theta_i^e\right]^{\mathrm{T}}$, $i = \mathrm{L}, 1 \cdots, n-1$ and $u_i(t) = [v_i \; w_i]^{\mathrm{T}}$ represents the inputs parameter of controller, while smooth nonlinear time-varying terms are constituted by $F_i(X_i(t)) = [v_{i-1}\cos\theta_i^e \; v_{i-1}\sin\theta_i^e \; w_{i-1}]^{\mathrm{T}}$ and $G_i(X_i(t)) = \begin{bmatrix} -1 & 0 & 0 \\ y_i^e & -x_i^e & -1 \end{bmatrix}^{\mathrm{T}}$.

Discretizing Eq. (3) with a sampling time of T_s yields. The Eq. (4) can be described as follows:

$$X_i(k+1) = A_i X_i(k) + B_i u_i(k) + h_i(X_i(k), u_i(k)) \tag{4}$$

wherein, $A_i = \frac{\partial F_i(X_i)}{\partial X_i}\Big|_{X_i=0,u_i=0}$, $B_i = \frac{\partial G_i(X_i)}{\partial X_i}\Big|_{X_i=0,u_i=0}$ and $h_i(X_i(k), u_i(k))$ are Lipschitz functions that satisfy the Lipschitz condition.

For the stable fleet system, control signal $u_i(k)$ is designed according to Eq. (4).

$$u_i(k) = C_i X_i(k) \tag{5}$$

Among them, $C_i = \begin{bmatrix} k_v & k_w \end{bmatrix}^{\mathrm{T}}$, $k_v = [\, k_{1v} \; k_{2v} \; k_{2v} \,]$, $k_w = [\, k_{1w} \; k_{2w} \; k_{2w} \,]$ are the controller gains to be designed.

2.2 Impacts of Sensor Failures

In this chapter, the consideration is given to the effects of sensor failures. The phenomena of distance, relative velocity, and sensor malfunctions between adjacent vehicles are described using the model employed in reference [10].

$$\begin{bmatrix} x_i^{fe}(k) & y_i^{fe}(k) & \theta_i^f \end{bmatrix} = \sigma_i \begin{bmatrix} x_i^e(k) & y_i^e(k) & \theta_i \end{bmatrix} \tag{6}$$

Under the influence of sensor failures, the actual measured output of the i-th autonomous vehicle is determined.

$$X_i^f(k) = \overline{\sigma}_i X_i(k) \tag{7}$$

To investigate the problem of convoy formation under the influence of sensor failures, the controller Eq. (5) can be rewritten as Eq. (8).

$$u_i^{\overline{\sigma}_i}(k) = C_i^{\overline{\sigma}_i} X_i(k) \tag{8}$$

Among them, $C_i^{\overline{\sigma}_i} = \sigma_i C_i$.

by substituting the controller Eq. (8) into Eq. (4), the convoy switching control system Eq. (9) can be obtained.

$$X_i(k+1) = A_i X_i(k) + B_i u_i^{\overline{\sigma}_i}(k) + h_i(X_i(k), u_i^{\overline{\sigma}_i}(k)) \tag{9}$$

This paper will propose a model predictive control method based on LMI, aiming to minimize the infinite-time performance index of the convoy system (9), where the index is defined by Eq. (10).

$$J_i = \sum_{r=0}^{\infty} X_{i(k+r|k)}^T Q_i X_{i(k+r|k)} + (u_{i(k+r|k)}^{\overline{\sigma}_i})^T R_i u_{i(k+r|k)}^{\overline{\sigma}_i} \tag{10}$$

Among them, $u_{i(k+r|k)}^{\overline{\sigma}_i} = (C_i^{\overline{\sigma}_i})_k X_{i(k+r|k)}$ and $(C_i^{\overline{\sigma}_i})_k$ are the state feedback controller gains at time k, Q_i is a positive definite matrix representing the state of the i-th

vehicle, R_i is a positive definite matrix representing the control input of the i-th vehicle, and r is the prediction for the next time step.

Assuming that the state feedback controller input is bounded, with a maximum allowed input of $u_{\max}$ and $u_{\max} \in \mathbb{R}$, Eq. (11) is derived.

$$\left\| u^{\overline{\sigma}_i}_{i(k+r|k)} \right\| \leq u_{\max} \tag{11}$$

The control objectives of this paper are achieved by the proposed nonlinear switching control method, which ensures lateral-longitudinal asymptotic stability and queue stability for the convoy.

3 Design of LMI-Based Model Predictive Controller

Theorem 3.1: According to the convoy system Eq. (4), H_i represents a lumped parameter nonlinear function, the existence of a differentiable function V_i and three continuously strictly increasing functions $\alpha_{im}(\cdot)(m = 1, 2, 3)$ is required to satisfy the following equations:

$$\begin{gathered} V_i(0) = 0 \\ \alpha_{i2}(\|X_i\|) \leq V_i(X_i) \leq \alpha_{i1}(\|X_i\|) \\ \Delta V_i = V_i(H_i(X_i)) - V_i(X_i) \leq -\alpha_{i3}(\|X_i\|) \end{gathered} \tag{12}$$

Thus, the asymptotic stability of the convoy in the Lyapunov sense is established. Building upon the previously mentioned lemma, the following sufficient conditions for the asymptotic stability of the nonlinear convoy system are formulated.

Theorem 3.2: Given a scalar $\alpha_i > 0$, $\mu_i > 0$, matrices $P_i^{\overline{\sigma}_i} > 0$, $R_i > 0$, $Q_i > 0$, $C_i^{\overline{\sigma}_i}$ and $M_i^{\overline{\sigma}_i}$ exist such that the following inequalities are satisfied:

$$\Delta_i = \begin{bmatrix} \Delta_i^1 & -\left(A_i + B_i C_i^{\overline{\sigma}_i}\right)^{\mathrm{T}} P_i^{\overline{\sigma}_i} \\ -P_i^{\overline{\sigma}_i}\left(A_i + B_i C_i^{\overline{\sigma}_i}\right) & \alpha_i P \end{bmatrix} \geq 0 \tag{13}$$

$$(1 + \alpha_i) h_i^{\mathrm{T}} h_i \leq X_i^{\mathrm{T}} M_i^{\overline{\sigma}_i} X_i \tag{14}$$

$$P_i^{\overline{\sigma}_i} \leq \mu_i I \tag{15}$$

When the nonlinear platoon communication network system encounters network attacks, ensuring the safe and stable operation of the nonlinear platoon requires the adoption of a resilient controller. This controller is designed to resist the impact of interferences and maintain the system parameters within a predefined safety range. Furthermore, in the event of a network attack, the resilient controller ensures that only local failures occur within the team control system, preventing the paralysis of the entire platoon system. Additionally, the resilient controller aims to restore the system to its normal state as quickly as possible.

Based on the aforementioned analysis, this study proposes the design of a resilient controller [13]:

$$\begin{aligned} u_i &= (K_i + \Delta K_i) a_{i(i-1)} \left(x_i\left(t_k^i h\right) - x_{i-1}\left(t_k^i h\right) \right), \\ t_k^i &\in \left[t_k^i h, t_{k+1}^i h \right) \end{aligned} \tag{16}$$

K_i represents the controller gain, while ΔK_i represents $C_i \Pi_i(t) H_i$. Ci and Hi are defined as given constant matrices. $\Pi_i(t)$ denotes an unknown time-varying matrix that must satisfy $\Pi_i^T(t)\Pi_i(t) \leq I$ [14, 15].

4 Analysis of String Stability

The condition for string stability is presented in the following theorem, based on the preceding analysis.

The following conditions are met for any $w > 0$:

$$\begin{cases} (a)\ 1 - 2E_a - 2E_v \eta_i > 0 \\ (b)\ E_\delta < 0 \end{cases} \tag{17}$$

String Stability of the Nonlinear Platoon System.

To establish the string stability of the nonlinear platoon system, we consider Eq. (16). In the event of a cyber-attack, the controller can be represented as follows:

$$u_i = (k_i + \Delta k_i) a_{i(i-1)} (x_i - x_{i-1}) \tag{18}$$

In the above formula, the parameters can be expressed as: $x_i(t) = [\,\delta_i\ v_i\ a_i\,]^T$,$k_i = \left[\,k_\delta\ k_v\ k_a\,\right]^T$,$\Delta k_i = \left[\,\Delta k_\delta\ \Delta k_v\ \Delta k_a\,\right]^T$.

The under expression can be obtained according to Eq. (7) under the condition of no interference and no resistance.

$$\dot{a}_i = -\frac{1}{\eta_i} a_i + \frac{1}{\eta_i} u_i \tag{19}$$

By bringing Eq. (18) into Eq. (19), the following expression can be obtained:

$$\begin{aligned} \dot{a}_i = -\frac{1}{\eta_i} a_i + \frac{1}{\eta_i} \big[& (k_\delta + \Delta k_\delta)(\delta_i - \delta_{i-1}) \\ & + (k_v + \Delta k_v)(v_i - v_{i-1}) \\ & + (k_a + \Delta k_a)(a_i - a_{i-1}) \big] \end{aligned} \tag{20}$$

Applying Laplace transform to both sides of Eq. (20) yields the following result:

$$\begin{aligned} \left[s - \left(\frac{k_a + \Delta k_a - 1}{\eta_i} \right) \right] a_i = & \frac{1}{\eta_i} \left[(k_\delta + \Delta k_\delta) \left(\frac{a_{i-1} - a_i}{s^2} \right) \right. \\ & \left. + (k_v + \Delta k_v) \left(\frac{a_{i-1} - a_i}{s} \right) \right. \end{aligned}$$

$$-(k_a + \Delta k_a)a_{i-1}\Big] \tag{21}$$

$$\begin{aligned} G(s) &= \frac{a_i(s)}{a_{i-1}(s)} \\ &= \frac{(k_\delta+\Delta k_\delta)+s(k_v+\Delta k_v)-s^2(k_a+\Delta k_a)}{s^3\eta_i-s^2(k_a+\Delta k_a-1)+s(k_v+\Delta k_v)+(k_\delta+\Delta k_\delta)} \end{aligned} \tag{22}$$

where $s = jw$, the under Eq. (23) is obtained:

$$G(jw) = \left|\frac{a_i(jw)}{a_{i-1}(jw)}\right| = \sqrt{\frac{a}{a+b}} \tag{23}$$

In the above formula, the parameters can be expressed as:

$$\Delta_i^1 = -Q_i - (C_i^{\overline{\sigma}_i})^{\mathrm{T}} R_i C_i^{\overline{\sigma}_i} - \mu_i M_i^{\overline{\sigma}_i} - \left(A_i + B_i C_i^{\overline{\sigma}_i}\right)^{\mathrm{T}} P_i^{\overline{\sigma}_i}\left(A_i + B_i C_i^{\overline{\sigma}_i}\right) + P_i^{\overline{\sigma}_i},\ \mu_i = \lambda_{\max}(P_i^{\overline{\sigma}_i})$$

Asymptotic stability is achieved by Eq. (17) of the nonlinear fleet switching system.
Proof: The Lyapunov function is defined for the system Eq. (17) as follows:

$$V_i(X_i) = X_i^{\mathrm{T}} P_i^{\overline{\sigma}_i} X_i \tag{24}$$

The following inequality is obtained due to $\Delta_i \geq 0$, wherein a positive definite symmetric matrix $P_i^{\overline{\sigma}_i}$ is involved.

$$\begin{aligned} &\left[X_i^{\mathrm{T}} h_i^{\mathrm{T}}\right]\Delta_i\begin{bmatrix} X_i \\ h_i \end{bmatrix} = -X_{i(k+r|k)}^{\mathrm{T}}\left(A_i + B_i C_i^{\overline{\sigma}_i}\right)^{\mathrm{T}} P_i^{\overline{\sigma}_i} A_i X_{i(k+r|k)} - X_{i(k+r|k)}^{\mathrm{T}}\left(A_i + B_i C_i^{\overline{\sigma}_i}\right)^{\mathrm{T}} * \\ &P_i^{\overline{\sigma}_i} B_i C_i^{\overline{\sigma}_i} X_{i(k+r|k)} - h_i^{\mathrm{T}} P_i^{\overline{\sigma}_i} A_i X_{i(k+r|k)} - h_i^{\mathrm{T}} P_i^{\overline{\sigma}_i} B_i C_i^{\overline{\sigma}_i} X_{i(k+r|k)} + \left(A_i X_{i(k+r|k)}\right)^{\mathrm{T}} P_i^{\overline{\sigma}_i} h_i - \\ &X_{i(k+r|k)}^{\mathrm{T}} * \left(B_i C_i^{\overline{\sigma}_i}\right)^{\mathrm{T}} P_i^{\overline{\sigma}_i} h_i - X_{i(k+r|k)}^{\mathrm{T}} P_i^{\overline{\sigma}_i} X_{i(k+r|k)} - X_{i(k+r|k)}^{\mathrm{T}} Q_i X_{i(k+r|k)} - \mu_i X_{i(k+r|k)}^{\mathrm{T}} M_i^{\overline{\sigma}_i} * \\ &X_{i(k+r|k)} - X_{i(k+r|k)}^{\mathrm{T}}\left(C_i^{\overline{\sigma}_i}\right)^{\mathrm{T}} R_i C_i^{\overline{\sigma}_i} X_{i(k+r|k)} + \alpha_i h_i^{\mathrm{T}} P_i^{\overline{\sigma}_i} h_i \geq 0 \end{aligned} \tag{25}$$

Then the following inequality can be gotten:

$$\begin{aligned} &[(A_i + B_i C_i^{\overline{\sigma}_i})X_{i(k+r|k)} + h_i]^{\mathrm{T}} P_i^{\overline{\sigma}_i}[(A_i + B_i C_i^{\overline{\sigma}_i})X_{i(k+r|k)} + h_i] - X_{i(k+r|k)}^{\mathrm{T}} P_i^{\overline{\sigma}_i} X_{i(k+r|k)} \leq \\ &-X_{i(k+r|k)}^{\mathrm{T}}(Q_i + \mu_i R_i B_i C_i^{\overline{\sigma}_i})X_{i(k+r|k)} + (1+\alpha_i)h_i^{\mathrm{T}} P_i^{\overline{\sigma}_i} h_i - \mu_i X_{i(k+r|k)}^{\mathrm{T}} M_i^{\overline{\sigma}_i} X_{i(k+r|k)} \end{aligned} \tag{26}$$

The Lyapunov function (24) in the convoy system, which represents the switching between sensor failure mode and normal mode, is expressed by the following equation, representing the increment of the left-hand side of inequality (26).

$$\begin{aligned} \Delta V_i = V_i(X_{i(k+r+1|k)}) - V_i(X_{i(k+r|k)}) \leq &-X_{i(k+r|k)}^{\mathrm{T}} Q_i X_{i(k+r|k)} - u_{i(k+r|k)}^{\mathrm{T}} R_i u_{i(k+r|k)} + \\ &(1+\alpha_i)h_i^{\mathrm{T}} P_i^{\overline{\sigma}_i} h_i - \mu_i X_{i(k+r|k)}^{\mathrm{T}} M_i^{\overline{\sigma}_i} X_{i(k+r|k)} \end{aligned} \tag{27}$$

To ensure the stability of the convoy switching system (17), the conditions stated in Lemma 3.2 regarding ΔV_i mentioned earlier need to be satisfied by $\alpha_{i3}(\cdot)$ that is sought.Based on Eq. (22), Eq. (23), and the provided $\mu_i = \lambda_{\max}(P_i^{\overline{\sigma}_i})$, Eq. (28) can be obtained.

$$(1+\alpha_i)h_i^{\mathrm{T}} P_i^{\overline{\sigma}_i} h_i \leq \mu_i X_i^{\mathrm{T}} M_i^{\overline{\sigma}_i} X_i \tag{28}$$

By bringing the above inequality formula (28) into inequality formula (27), we can get:

$$\Delta V_i \leq -X^{\mathrm{T}}_{i(k+r|k)} Q_i X_{i(k+r|k)} - u^{\mathrm{T}}_{i(k+r|k)} R_i u_{i(k+r|k)} \tag{29}$$

According to formula (26), the following three strictly increasing functions can be obtained:

$$\begin{aligned} \alpha_{i1}(\|X_i\|) &= \max \lambda_{\max}\left(P_i^{\overline{\sigma}_i}\right)\|X_i\|^2 \\ \alpha_{i2}(\|X_i\|) &= \min \lambda_{\min}\left(P_i^{\overline{\sigma}_i}\right)\|X_i\|^2 \\ \alpha_{i3}(\|X_i\|) &= \min \lambda_{\min}\left(Q_i + (C_i^{\overline{\sigma}_i})^{\mathrm{T}} R_i C_i^{\overline{\sigma}_i}\right)\|X_i\|^2 \end{aligned} \tag{30}$$

The conditions stated in Theorem 3.1 are fulfilled, thereby ensuring that the nonlinear fleet switching system maintains asymptotic stability even in the event of sensor failure.

Theorem 3.1 encompasses adequate conditions for achieving asymptotic stability in the nonlinear fleet switching system. To further enhance fleet control performance, the stability model predictive control method provided in Eq. (18) is employed to minimize the infinite time domain performance index of the fleet. The solution theorem for the optimization problem is presented as follows:

The conditions stated in Theorem 3.1 are met, thus proving that the nonlinear platoon switching system can still achieve asymptotic stability in the presence of sensor faults. Sufficient conditions for asymptotic stability of the nonlinear platoon switching system are provided by Theorem 3.1. To enhance the control performance of the platoon, an optimization problem is formulated utilizing the stable model predictive control method presented in Eq. (18).

Theorem 3.3: Design feedback controller $u_{i(k+r|k)} = C_i^{\overline{\sigma}_i} X_{i(k+r|k)}$, $r \geq 0$, for the nonlinear platoon switching system (Eq. (17)) such that $C_i^{\overline{\sigma}_i} = Y_i (Q_i^{\overline{\sigma}_i})^{-1}$ minimizes the performance index function given in Eq. (18). The matrices Y_i and $Q_i^{\overline{\sigma}_i}$ satisfy the following LMI optimization problem.

$$\min \ \gamma_i$$

$$\text{Subject to:} \begin{bmatrix} I & X^T_{i(k|k)} \\ X_{i(k|k)} & Q_i^{\overline{\sigma}_i} \end{bmatrix} > 0 \tag{31}$$

$$\Delta_i = \begin{bmatrix} Q_i^{\overline{\sigma}_i} & -(A_i Q_i^{\overline{\sigma}_i} + B_i Y_i)^{\mathrm{T}} & Q_i^{\overline{\sigma}_i} & 0 & Y_i^{\mathrm{T}} & 0 & Q_i^{\overline{\sigma}_i} & 0 & (A_i Q_i^{\overline{\sigma}_i} + B_i Y_i)^{\mathrm{T}} & 0 \\ * & \alpha_i Q_i^{\overline{\sigma}_i} & 0 & 0 & 0 & 0 & 0 & 0 & 0 & 0 \\ * & * & \gamma_i (Q_i^{\overline{\sigma}_i})^{-1} & 0 & 0 & 0 & 0 & 0 & 0 & 0 \\ * & * & * & \gamma_i (Q_i^{\overline{\sigma}_i})^{-1} & 0 & 0 & 0 & 0 & 0 & 0 \\ * & * & * & * & \gamma_i R_i^{-1} & 0 & 0 & 0 & 0 & 0 \\ * & * & * & * & * & \gamma_i R_i^{-1} & 0 & 0 & 0 & 0 \\ * & * & * & * & * & * & \beta_i (M_i^{\overline{\sigma}_i})^{-1} & 0 & 0 & 0 \\ * & * & * & * & * & * & * & \beta_i (M_i^{\overline{\sigma}_i})^{-1} & 0 & 0 \\ * & * & * & * & * & * & * & * & Q_i^{\overline{\sigma}_i} & 0 \\ * & * & * & * & * & * & * & * & * & Q_i^{\overline{\sigma}_i} \end{bmatrix} > 0 \tag{32}$$

$$\begin{bmatrix} u^2_{\max} I & Y_i \\ Y_i^{\mathrm{T}} & Q_i^{\overline{\sigma}_i} \end{bmatrix} > 0 \tag{33}$$

$$Q_i^{\overline{\sigma}_i} - \beta_i I > 0 \tag{34}$$

Proof: The inequality (29) is proven by adding both sides from $r = 0$ to $r = \infty$.

$$\lim_{r\to\infty}\left[X_{i(k+r|k)}^{\mathrm{T}} P_i^{\overline{\sigma}_i} X_{i(k+r|k)}\right] - X_{i(k|k)}^{\mathrm{T}} P_i^{\overline{\sigma}_i} X_{i(k|k)} \le -J_i \tag{35}$$

The stability of the system indicates that Equation $\lim_{k\to\infty} X_k = 0$, thus the aforementioned inequality (35) can be expressed as:

$$J_i^* = J_i \le X_{i(k|k)}^{\mathrm{T}} P_i^{\overline{\sigma}_i} X_{i(k|k)} \tag{36}$$

J_i^* represents the upper bound of the objective function.

The minimization criterion function is aimed to be satisfied by the designed $u_{i(k+r|k)}$ in order to fulfill the optimization objective, considering the following optimization problem.

$$\begin{aligned} &\min \gamma_i \\ &\text{Subject to: } X_{i(k|k)}^{\mathrm{T}} P_i^{\overline{\sigma}_i} X_{i(k|k)} < \gamma_i \end{aligned} \tag{37}$$

By utilizing the Schur complement theorem and defining $P_i^{\overline{\sigma}_i} = \gamma_i (Q_i^{\overline{\sigma}_i})^{-1}$, Eq. (31) can be obtained.

$$\begin{aligned} &\min \gamma_i \\ &\text{Subject to: } \begin{bmatrix} I & X_{i(k|k)}^{\mathrm{T}} \\ X_{i(k|k)} & Q_i^{\overline{\sigma}_i} \end{bmatrix} > 0 \end{aligned}$$

The inequality (13) is multiplied on both sides by $diag\{\, Q_i^{\overline{\sigma}_i}, Q_i^{\overline{\sigma}_i} \}$ and γ_i^{-1}, defining $C_i^{\overline{\sigma}_i} = Y_i (Q_i^{\overline{\sigma}_i})^{-1}$, $P_i^{\overline{\sigma}_i} = \gamma_i (Q_i^{\overline{\sigma}_i})^{-1}$, and $\mu_i^{-1}\gamma_i = \beta_i$, Then, The Following inequality is obtained.

$$\begin{bmatrix} \overline{\Delta}_i & -(A_i Q_i^{\overline{\sigma}_i} + B_i Y_i)^{\mathrm{T}} \\ -(A_i Q_i^{\overline{\sigma}_i} + B_i Y_i) & \alpha_i Q_i^{\overline{\sigma}_i} \end{bmatrix} \ge 0 \tag{38}$$

Wherein,

$$\overline{\Delta}_i = -\gamma_i^{-1} Q_i^{\overline{\sigma}_i} Q_i Q_i^{\overline{\sigma}_i} - \gamma_i^{-1} Y_i^{\mathrm{T}} R_i Y_i - \beta_i^{-1} Q_i^{\overline{\sigma}_i} M_i^{\overline{\sigma}_i} Q_i^{\overline{\sigma}_i} - \left(A_i Q_i^{\overline{\sigma}_i} + B_i Y_i\right)^{\mathrm{T}} P_i^{\overline{\sigma}_i} \left(A_i Q_i^{\overline{\sigma}_i} + B_i Y_i\right) + Q_i^{\overline{\sigma}_i}$$

Based on Eq. (38), the optimization conditions given by the Schur complement theorem and Eq. (33), it can be proven that Eq. (29) holds.

In order to prove condition (22), the input of the state feedback controller (11) is considered, and $P_i^{\overline{\sigma}_i} = \gamma_i (Q_i^{\overline{\sigma}_i})^{-1}$ is substituted into Eq. (37).

$$X_{i(k|k)}^{\mathrm{T}} (Q_i^{\overline{\sigma}_i})^{-1} X_{i(k|k)} < 1 \tag{39}$$

Consequently, the following inequation can be obtained.

$$\left\| (Q_i^{\overline{\sigma}_i})^{-0.5} X_{i(k+r|k)} \right\|_2^2 < 1 \tag{40}$$

According to $u_{i(k+r|k)}^{\overline{\sigma}_i} = (C_i^{\overline{\sigma}_i})_k X_{i(k+r|k)}$, $C_i^{\overline{\sigma}_i} = Y_i (Q_i^{\overline{\sigma}_i})^{-1}$ and formula (40), the norm of controller input 2 can obtain:

$$\left\|u_{i(k+r|k)}\right\|_2^2 = \left\|(C_i^{\overline{\sigma}_i})_k X_{i(k+r|k)}\right\|_2^2 = \left\|Y(Q_i^{\overline{\sigma}_i})^{-0.5}((Q_i^{\overline{\sigma}_i})^{-0.5} X_{i(k+r|k)})\right\|_2^2 < \left\|Y(Q_i^{\overline{\sigma}_i})^{-0.5}\right\|_2^2 \tag{41}$$

According to formula (33) and formula (11), formula (42) can be derived.

$$Y_i^{\mathrm{T}}(Q_i^{\overline{\sigma}_i})^{-1} Y_i - u_{\max}^2 I < 0 \tag{42}$$

From formula (42), according to Schur's complement theorem, formula (30) can be established. At the same time, by bringing $\beta_i = u_i^{-1}\gamma_i$ and $P_i^{\overline{\sigma}_i} = \gamma_i (Q_i^{\overline{\sigma}_i})^{-1}$ into the equation of inequality (15), we can get

$$Q_i^{\overline{\sigma}_i} - \beta_i I > 0$$

Therefore, formula (34) is established and verified.

5 The Stability Analysis of the Fleet

In this section, the fleet stability objective of the platoon is analyzed based on controller (5). Firstly, an analysis is conducted on the fleet stability goals of the platoon, according to the platoon's controller, formula (43) can be derived.

$$u_i^{\overline{\sigma}_i}(t) = \begin{bmatrix} k_{1v} x_i^e(t) + k_{2v} y_i^e(t) + k_{3v}\theta_i^e(t) \\ k_{1w} x_i^e(t) + k_{2w} y_i^e(t) + k_{3w}\theta_i^e(t) \end{bmatrix} \sigma_i \tag{43}$$

Then, the following can be gotten.

$$\begin{cases} a_{xi} = (\sigma_i k_{1v}\dot{x}_i^e(t) + \sigma_i k_{2v}\dot{y}_i^e(t) + \sigma_i k_{3v}\dot{\theta}_i^e(t))\cos\theta_i \\ \quad -(\sigma_i k_{1v} x_i^e(t) + \sigma_i k_{2v} y_i^e(t) + \sigma_i k_{3v}\theta_i^e(t))\sin\theta_i \\ a_{yi} = (\sigma_i k_{1v}\dot{x}_i^e(t) + \sigma_i k_{2v}\dot{y}_i^e(t) + \sigma_i k_{3v}\dot{\theta}_i^e(t))\sin\theta_i \\ \quad +(\sigma_i k_{1v} x_i^e(t) + \sigma_i k_{2v} y_i^e(t) + \sigma_i k_{3v}\theta_i^e(t))cos\theta_i \end{cases} \tag{44}$$

In order to simplify the calculation process, it is assumed from an academic perspective that the autonomous vehicles travel in a two-dimensional plane, and the steering angle of the autonomous vehicle is considered a constant value denoted as $\theta_i = -\pi/4$. When $a_{xi} = a_{yi}$, formula (45) can be derived.

$$\dot{a}_i(t) = \frac{\sqrt{2}}{2}(\sigma_i k_{1v}\dot{x}_i^e(t) + \sigma_i k_{2v}\dot{y}_i^e(t))\sin\theta_i(t) + (\sigma_i k_{1v} x_i^e(t) + \sigma_i k_{2v} y_i^e(t)) \tag{45}$$

wherein, $a_i = a_{xi} = a_{yi}$,The equation is Laplace transformed, and $a_i(0) = 0$ is assumed in order to obtain:

$$a_i(s) = \frac{\sqrt{2}}{2}(\sigma_i s + 1)(k_{1v} x_i^e(s) + k_{2v} y_i^e(s)) \tag{46}$$

According to formula (2), the following formula can be obtained.

$$x_i^e(s) = y_i^e(s) = \frac{\sqrt{2}}{2}(x_{i-1}(s) - x_i(s)) + (y_{i-1}(s) - y_i(s)) \tag{47}$$

Furthermore

$$x_i(s) = y_i(s) = \frac{1}{s^2}a_i(s) \tag{48}$$

By combining Eqs. (47) and (48), and substituting them into Eq. (46), the following is obtained.

$$a_i(s) = \frac{1}{2}(\sigma_i s + 1)(k_{1v} + k_{2v})(x_{i-1}(s) - x_i(s)) = \frac{1}{2}(\sigma_i s + 1)(k_{1v} + k_{2v})\frac{1}{s^2}(a_{i-1}(s) - a_i(s)) \tag{49}$$

Subsequently, the following can be derived.

$$\begin{aligned}(s^2 + \tfrac{1}{2}(\sigma_i s^3 + s^2)(k_{1v} + k_{2v}))a_i(s) &= \tfrac{1}{2}(\sigma_i s^3 + s^2)(k_{1v} + k_{2v})a_{i-1}(s) \\ &= \tfrac{1}{2}(\sigma_i s^3 + s^2)(k_{1v} + k_{2v})a_{i-1}(s) \\ G(s) = \frac{a_i(s)}{a_{i-1}(s)} &= \frac{\sigma_i s^3 + s^2}{\sigma_i s^3 + (1 + 2/(k_{1v} + k_{2v}))s^2}\end{aligned} \tag{50}$$

In order to satisfy the requirement of stable queue formation for the fleet, i.e., ensuring that $\left|a_i(jw)/a_{i-1}(jw)\right| \leq 1$ holds for any $w > 0$, further processing is carried out on the above equation.

$$G(jw) = \left|\frac{a_i(jw)}{a_{i-1}(jw)}\right| = \sqrt{\frac{1 + (\sigma_i w)^2}{1 + (\sigma_i w)^2 + 4/(k_{1v} + k_{2v}) + 4/(k_{1v} + k_{2v})^2}} \tag{51}$$

Due to the inequality $1 + (\sigma_i w)^2 > 0$, it follows that as long as the inequality $1/(k_{1v} + k_{2v}) + 1/(k_{1v} + k_{2v})^2 > 0$ is satisfied, the inequality $\left|a_i(jw)/a_{i-1}(jw)\right| \leq 1$ holds when the inequality $k_{1v} + k_{2v} > -1$ is met. Through the aforementioned analysis, it is verified that the proposed controller in this chapter can meet the requirement of stable queue formation for the fleet.

6 Experimental Analysis

For the purpose of conducting safe experiments in the laboratory, the previously mentioned fleet system is downscaled in a 1:20 ratio. The experimental platform comprises three small unmanned vehicles, as depicted in Fig. 2.

Arduino serves as the main control unit, while the distance between two adjacent vehicles is measured using an infrared sensor. The model car is equipped with a speed sensor, an accelerometer, a WiFi module, and other accessories. These sensors are utilized to measure the speed and acceleration of the equipped unmanned vehicle, and the information is transmitted to the following unmanned vehicle through the WiFi module.Using Bernoulli sequence to simulate the operation mode of the sensor during a period [0, 35s], the probability of normal operation state $\sigma = 1$ is 95%, and the probability of failure operation state $\sigma = 0$ is 5%, with d = 10 cm.The performance of the

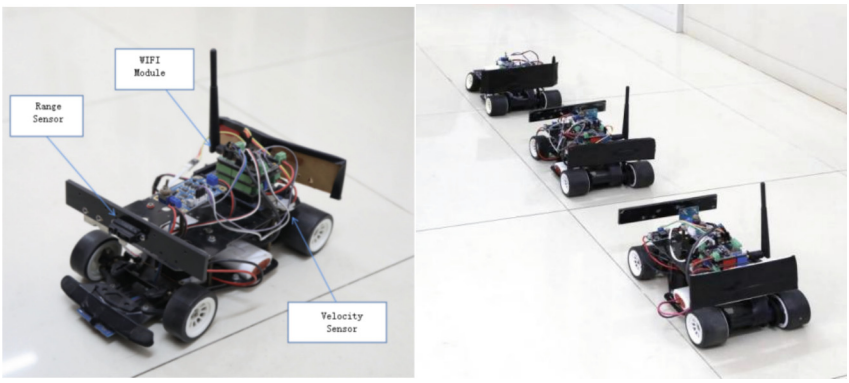

Fig. 2. Experimental vehicles and formation system

proposed controller algorithm is examined from an academic perspective by conducting tests in two practical scenarios.

Scenario One: Three Vehicles Traveling in a Straight Line.

In the experiment, the lead vehicle and the following vehicle start traveling along a plane from an initial velocity of 0 m/s. The lead vehicle accelerates to velocity $v_L = 16$cm/s, after which it maintains a constant speed. In this scenario, the following unmanned vehicle aims to match the expected velocity of the lead vehicle under condition $w_L = 0$.

It is demonstrated by the experimental results that the excellent performance of the proposed controller. The trajectory of the vehicle fleet is observed to be relatively smooth, and the lead vehicle is accurately tracked at the desired speed by all the following unmanned vehicles, as depicted in Fig. 3(a). By contrast, when using the control algorithm from reference [9] in the same scenario (as shown in Fig. 3b)), the motion trajectory and velocity of the unmanned vehicles exhibit significant fluctuations. The maximum inter-vehicle distance is 0.752 m.

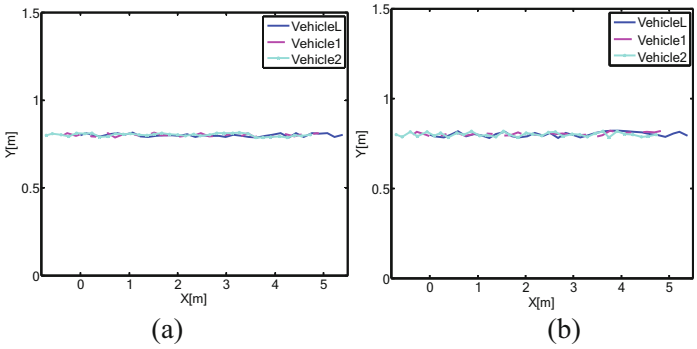

Fig. 3. Circular Road Travel with Three Vehicles: a) Trajectory of the Vehicle Fleet; b) Trajectory of the Vehicle Fleet in [9].

Scenario Two: Three Vehicles Traveling on a Circular Road.

In the experiment, the lead vehicle and the following vehicle start traveling on a circular track from an initial velocity of 0 cm/s. The lead vehicle accelerates to velocity $v_L = 16$ cm/s, after which it maintains a constant speed. In this scenario, the following unmanned vehicle aims to match the expected velocity of the lead vehicle.

The designed controller in this study exhibits excellent performance. Even in the event of sensor failures within the vehicle fleet, the vehicles can still follow the desired trajectory. The trajectory of the vehicle fleet remains relatively smooth, achieving asymptotic stability and queue stability. However, when using the controller from reference [9], errors accumulate due to sensor failures, resulting in instability in the third vehicle. This leads to significant tracking errors and poorer control performance, as shown in Fig. 4.

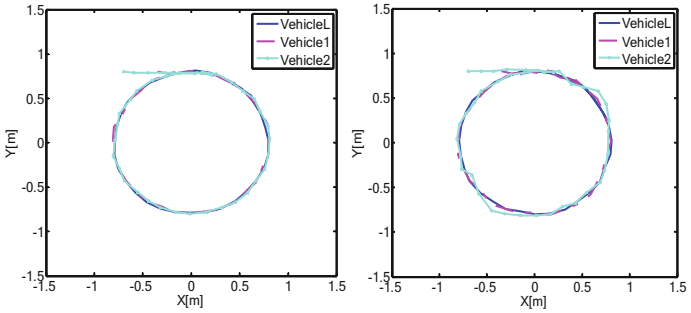

Fig. 4. Circular Road Travel with Three Vehicles: a) Trajectory of the Vehicle Fleet; b) Trajectory of the Vehicle Fleet in [9].

7 Conclusions

A model predictive control method based on LMI is proposed in this paper for achieving coordinated formation control of unmanned vehicles. The stable operation of the convoy is ensured even in the presence of sensor failures, leading to satisfactory control performance. The effectiveness of the algorithm is experimentally validated, with emphasis on considering faults specifically in onboard sensors. The investigation does not encompass network-induced factors. Future research will concentrate on studying the problem of coordinated formation control of unmanned vehicles under simultaneous failures in both sensor and wireless communication systems.

Acknowledgment. This work was supported by National Natural Science Foundation of China Project (51077125) and Beijing Institute Of Technology, Zhuhai Project (2023058ZLGC). Thanks for all the persons who gave me assistances in the course of experiment and writing.

References

1. Wang, C., Chen, K., Hao, J.: A model predictive control approach for vehicle formation tracking with input saturation. IEEE Trans. Intell. Transp. Syst. **22**(3), 1715–1726 (2022)
2. Yang, X., Li, B., Duan, F., Pan, Y.: Distributed model predictive formation control of connected vehicles with adaptive communication topologies. IEEE Trans. Intell. Transp. Syst. **21**(12), 5164–5177 (2022)
3. Li, W., Cheng, Y., Jiang, Z.P.: Robust formation control for autonomous vehicles with uncertain dynamics and limited communication. Automatica **115**, 108879 (2020)
4. Zhang, H., Liu, H., Wu, Q.J.: Consensus-based distributed model predictive control for vehicle formations. IEEE Trans. Intell. Transp. Syst. **20**(3), 1027–1038 (2022)
5. Huang, Y., Liu, Y., Zheng, N.: Distributed adaptive formation control of multiple autonomous underwater vehicles with unknown dynamics. IEEE Trans. Ind. Electron. **66**(7), 5270–5280 (2022)
6. Li, F., Xia, Y., Rees, D.: Model predictive formation control for multi-agent systems. Int. J. Robust Nonlinear Control **28**(18), 5686–5702 (2018)
7. Wang, R., Li, L., Yu, J., Sun, Y.: Distributed adaptive containment control for multi-agent systems with unknown time-varying delays and high-order dynamics. IEEE Trans. Cybern. **50**(4), 1639–1650 (2018)
8. Zhang, H., Wu, Q.J., Liu, H.: A distributed model predictive control approach for vehicle platoon control. Transport. Res. Part C: Emerg. Technol. **75**, 143–159 (2017)
9. Kang, W., Xie, G.M., Wang, L., Huang, T.: Cooperative trajectory tracking of multiple surface vessels with input saturation based on model predictive control. Ocean Eng. **135**, 1–10 (2017)
10. Liang, H., Dong, Y., Cheng, L.: Model predictive formation control for leader-follower multiagent systems. IEEE Trans. Control Syst. Technol. **24**(2), 685–692 (2016)
11. Zhou, X., Ji, M.: Model predictive formation control of multiple unmanned aerial vehicles with collision avoidance. J. Intell. Rob. Syst. **102**(2), 39–51 (2022)
12. Li, J., Chen, Y., Huang, Y.: Distributed model predictive control for leader-follower formation control of multi-agent systems. IEEE Trans. Ind. Inf. **16**(8), 5287–5296 (2022)
13. Yang, Z., Zhang, L., Jin, Y.: Distributed formation control for nonholonomic mobile robots via model predictive control. Robot. Auton. Syst. **130**, 103616 (2020)
14. Zhang, J., Liu, Y., Zheng, N.: Adaptive distributed formation control of autonomous vehicles with a virtual leader. IEEE Trans. Veh. Technol. **68**(5), 4468–4481 (2019)
15. Li, S., Jiang, B., Zhang, C.: Consensus-based distributed model predictive control for multi-vehicle formations under directed graphs. Int. J. Robust Nonlinear Control **28**(14), 4286–4304 (2018)
16. Ma, X., Ning, B., Tian, Y.: Leader-following formation control of networked nonholonomic mobile robots with model predictive control approach. IEEE Trans. Ind. Inf. **13**(3), 953–962 (2017)
17. Ren, W., Beard, R.W.: Consensus seeking in multiagent systems under dynamically changing interaction topologies. IEEE Trans. Autom. Control **60**(1), 65–77 (2015)
18. Yang, T., Li, H., Dong, Y.: Dynamic formation control of nonholonomic mobile robots using output feedback model predictive control. IEEE Trans. Ind. Electron. **61**(7), 3526–3535 (2014)
19. Gao, J., Wang, L., Xie, L.: Model predictive control based formation control for multi-agent systems with input constraints. Automatica **49**(9), 2730–2738 (2013)
20. Olfati-Saber, R., Fax, J.A., Murray, R.M.: Consensus and cooperation in networked multi-agent systems. Proc. IEEE **95**(1), 215–233 (2007)